

Zirconium-promoted hydrothermal synthesis of hierarchical porous carbons with ordered cubic mesostructure under acidic aqueous condition

Anfeng Zhang^a, Keke Hou^b, Haiyang Duan^a, Wei Tan^b, Chunshan Song^{a,d*} and Xinwen Guo^{a,*}

Received 00th January 20xx,
Accepted 00th January 20xx

DOI: 10.1039/x0xx00000x

www.rsc.org/

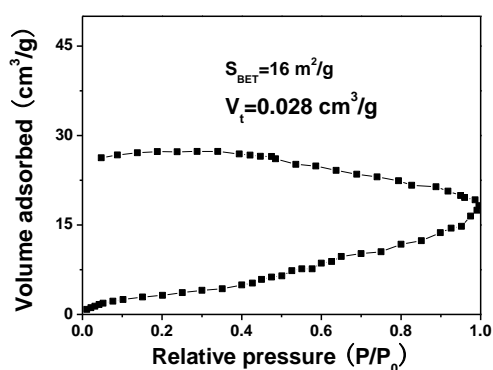


Fig. S1 Nitrogen adsorption-desorption isotherms of OMC1-0.04-2-400.

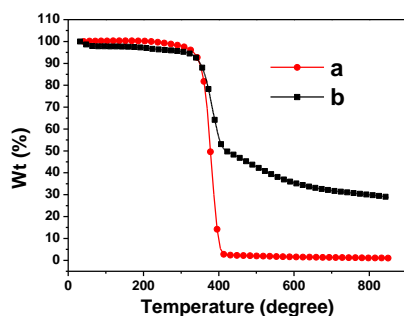


Fig. S2 TG curves of F127 (a) and the as-made OMC1-0.04-2-600 (b).

As shown in Fig. S2b, the weight loss of the as-made OMC1-0.04-2-600 can be divided into three stages. At the first stage between 320 and 400 °C, the weight loss reached to 45%, due to the decomposition of the surfactant F127 (in Fig. S2a). The second one between 400 and 600 was contributed much to the decomposition of the polymer framework. The weight loss above 600 °C was mainly due to the continuous decomposition of the carbon framework.

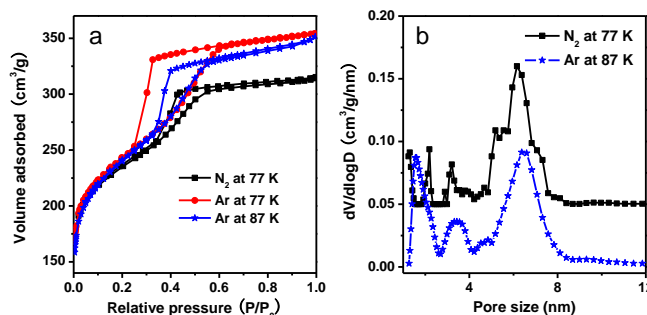


Fig. S3 Nitrogen (77 K) and Argon (87 and 77 K) sorption isotherms (a) and pore size distributions (b) calculated by the adsorption branch of the nitrogen (77 K) and argon (87 K) sorption isotherms with cylindrical-spherical adsorption kernel of OMC1-0.04-2-600.

^a State Key Lab of Fine Chemicals, PSU-DUT Joint Center for Energy Research, School of Chemical Engineering, Dalian University of Technology, Dalian 116024, P. R. China. Fax: 86-0411-86986134; Tel: 86-0411-86986133; E-mail: Guoxw@dlut.edu.cn

^b Chambroad Chemical Industry Research Institute Co., LTD, Binzhou, Shandong, P. R. China.

^c EMS Energy Institute, PSU-DUT Joint Center for Energy Research, Department of Energy & Mineral Engineering, and Department of Chemical Engineering Pennsylvania State University, University Park, Pennsylvania 16802, United States. Fax: 814-865-3573; Tel: 814-863-4466; E-mail: csong@psu.edu

Electronic Supplementary Information (ESI) available: [details of any supplementary information available should be included here]. See DOI: 10.1039/x0xx00000x

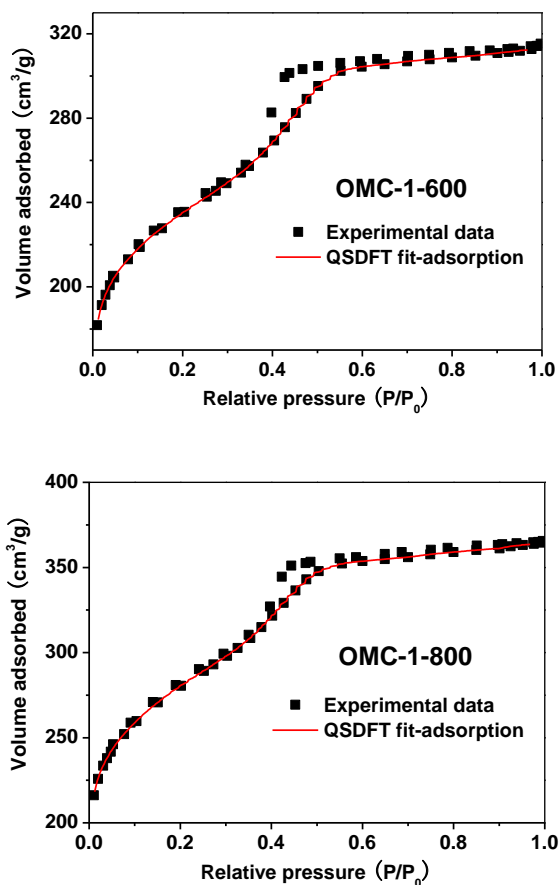


Fig. S4 Experimental nitrogen sorption isotherms with fit from QSDFT cylindrical-spherical adsorption model for the samples pyrolyzed at 600 and 800 °C.

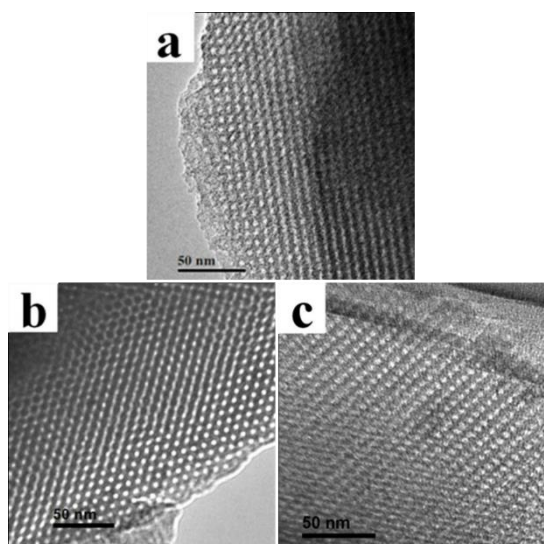


Fig. S5 TEM images viewed along: (a) [100], (b) [111], and (c) [110] directions for the sample synthesized in the absence of $ZrOCl_2 \cdot 8H_2O$ (from the top layer of the autoclave).

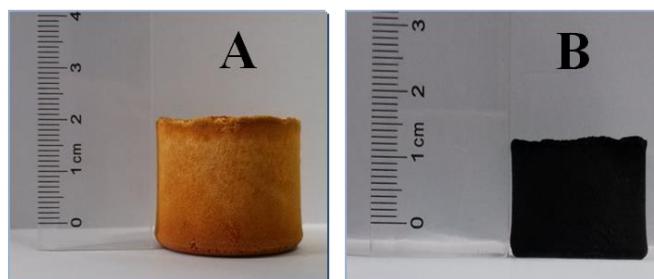


Fig. S6 Photographs of the synthesized polymer and carbon monoliths.

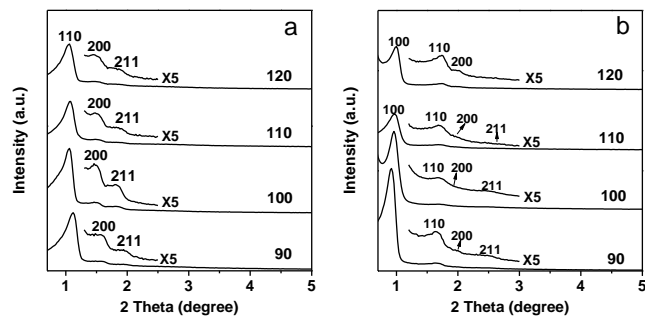


Fig. S7 XRD patterns of OMC1-0.04-2-600 (a) and OMC2-0.04-2-600 (b) synthesized at different temperatures.

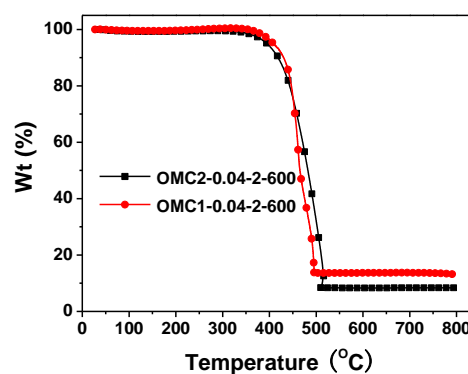


Fig. S8 TG curves of OMC1-0.04-2-600 and OMC2-0.04-2-600.

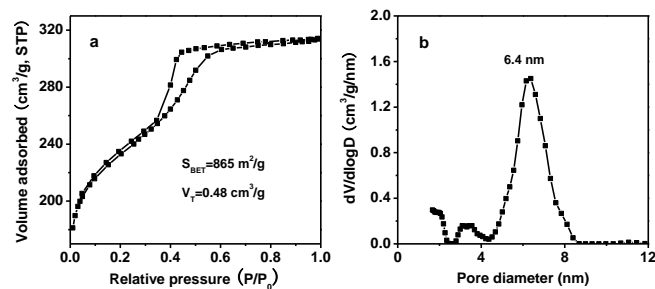


Fig. S9 Nitrogen sorption isotherms (a) and the corresponding pore size distributions (b) of sample OMC1-0.04-2-600 synthesized in large scale by a factor of 20.

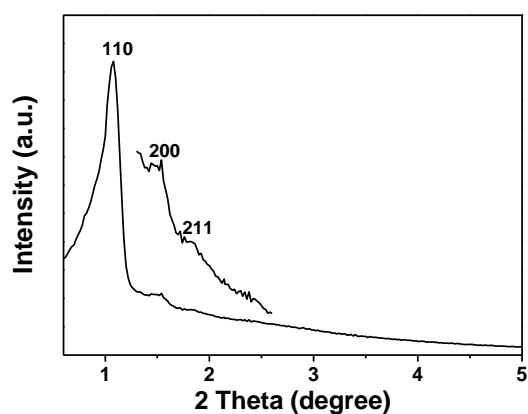


Fig. S10 The XRD pattern of OMC1-0.04-2-600 synthesized in large scale by a factor of 20.

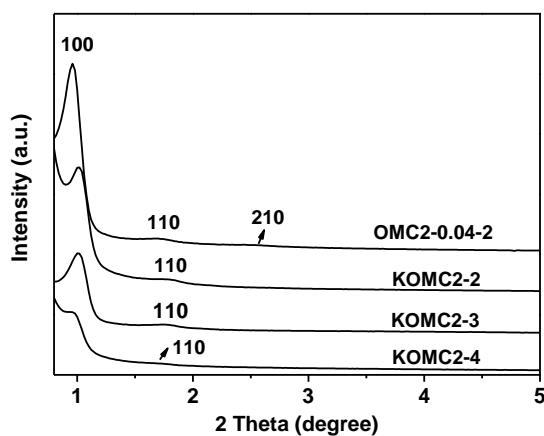


Fig. S11 XRD patterns of OMC2-0.04-2-600 and the activated samples with various KOH/carbon mass ratios.

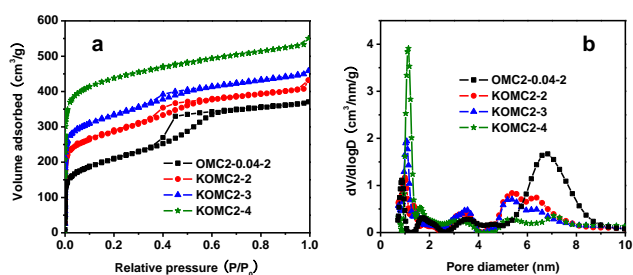


Fig. S12 Nitrogen sorption isotherms (a) and pore size distributions (b) of OMC2-0.04-2-600 and the activated samples with various KOH/carbon mass ratios.

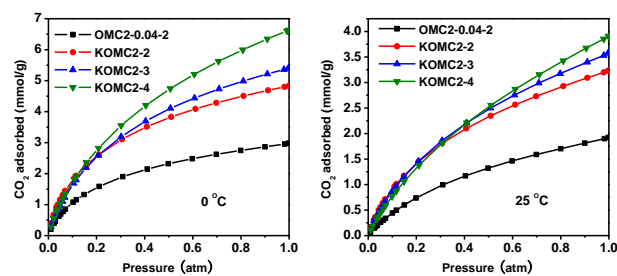


Fig. S13 CO₂ sorption isotherms of OMC2-0.04-2-600 and the activated samples with various KOH/carbon mass ratios.